

## Article

# Food-Derived Bioactive Peptides with Antioxidative Capacity, Xanthine Oxidase and Tyrosinase Inhibitory Activity

Anthony Thaha <sup>1</sup>, Bor-Sen Wang <sup>2</sup>, Yu-Wei Chang <sup>1,3</sup>, Shih-Min Hsia <sup>4</sup> , Tsui-Chin Huang <sup>5</sup> ,  
Chyuan-Yuan Shiau <sup>1</sup>, Deng-Fwu Hwang <sup>1</sup> and Tai-Yuan Chen <sup>1,\*</sup> 

<sup>1</sup> Department of Food Science, Center of Excellence for the Oceans, National Taiwan Ocean University, Keelung 20224, Taiwan; anthonythaha@gmail.com (A.T.); bweichang@email.ntou.edu.tw (Y.-W.C.); cyshiau@mail.ntou.edu.tw (C.-Y.S.); dfhwang@mail.ntou.edu.tw (D.-F.H.)

<sup>2</sup> Department of Applied Life Science & Health, Chia-Nan University of Pharmacy and Science, Tainan 71710, Taiwan; wangbs@mail.cnu.edu.tw

<sup>3</sup> Institute of Food Safety and Risk Management, National Taiwan Ocean University, Keelung 20224, Taiwan

<sup>4</sup> School of Nutrition and Health Sciences, College of Nutrition, Taipei Medical University, Taipei 11031, Taiwan; bryanhsia@tmu.edu.tw

<sup>5</sup> Graduate Institute of Cancer Biology and Drug Discovery, College of Medical Science and Technology, Taipei Medical University, Taipei 11031, Taiwan; tsuichin@tmu.edu.tw

\* Correspondence: tychen@email.ntou.edu.tw; Tel.: +886-2-24622192 (ext. 5124); Fax: +886-2-24628750

**Abstract:** Bioactive peptides (BPs) released by proteases from different food protein sources are often served as antioxidants in food applications. This study aims to investigate 11 BPs derived from fish and egg white as potential natural antioxidants by antioxidant activity assays. The kinetic activity of the BPs against xanthine oxidase (XOD) and tyrosinase was also analyzed. The antioxidative capacity of the BPs indicated that VWWW (VW4, mackerel meat), followed by IRW (IW3, egg white) and VKAGFAWTANQQLS (VS14, tuna backbone protein), possessed the highest antioxidant activity in 1,1-diphenyl-2-picrylhydrazyl radical (DPPH), 2,2'-azino-bis(3-ethylbenzothiazoline-6-sulfonic acid) diammonium salt (ABTS) and reducing power (RP) assays. Both the free-radical scavenging score predicted from the AnOxPePred algorithm and the DPPH, ABTS and RP results indicated that VW4 was the best antioxidant. Furthermore, the XOD and tyrosinase inhibition by three selected peptides exhibited competitive patterns of effective inhibition. The half maximal inhibitory concentrations (IC<sub>50</sub>) of the peptides for XOD inhibition were 5.310, 3.935, and 1.804 mM for VW4, IW3, and VS14, respectively, and they could serve as competitive natural XOD inhibitors. The IC<sub>50</sub> of the peptides for tyrosinase inhibition were 1.254, 2.895, and 0.595 mM for VW4, IW3, and VS14, respectively. Overall, VW4, IW3, and VS14 are potential antioxidants and natural XOD inhibitors for preventing milk-fat oxidation, and anti-browning sources for inhibiting food-derived tyrosinase oxidation.

**Keywords:** bioactive peptides; antioxidant; xanthine oxidase; tyrosinase; anti-browning; enzyme kinetics



**Citation:** Thaha, A.; Wang, B.-S.; Chang, Y.-W.; Hsia, S.-M.; Huang, T.-C.; Shiau, C.-Y.; Hwang, D.-F.; Chen, T.-Y. Food-Derived Bioactive Peptides with Antioxidative Capacity, Xanthine Oxidase and Tyrosinase Inhibitory Activity. *Processes* **2021**, *9*, 747. <https://doi.org/10.3390/pr9050747>

Academic Editor: Dariusz Dziki

Received: 16 March 2021

Accepted: 21 April 2021

Published: 23 April 2021

**Publisher's Note:** MDPI stays neutral with regard to jurisdictional claims in published maps and institutional affiliations.



**Copyright:** © 2021 by the authors. Licensee MDPI, Basel, Switzerland. This article is an open access article distributed under the terms and conditions of the Creative Commons Attribution (CC BY) license (<https://creativecommons.org/licenses/by/4.0/>).

## 1. Introduction

Reactive oxygen species (ROS) overproduction and oxidative stress can damage the endogenous antioxidant defense system. The free radicals have serious pathological consequences on biomacromolecules such as DNA, proteins, and lipids, which leads to the initiation and progression of numerous health disorders, including inflammation, diabetes, gout, neurodegenerative diseases, cardiovascular diseases, and cancer [1]. Moreover, free-radical-mediated lipid oxidation can cause serious deterioration in food quality, gustatory appeal, nutrition, and safety by reacting with volatile compounds, amino acids, proteins, vitamins, and cholesterol [2]. Many synthetic food additives (antioxidants) such as butylated hydroxytoluene (BHT), butylated hydroxyanisole (BHA), tert-butylhydroquinone (TBHQ), and propyl gallate (PG) are widely used in most countries to protect food quality

from peroxidation and auto-oxidation processes [2,3]. However, use of these synthetic antioxidants must be strictly controlled under legal regulation because of safety concerns [3]. Antioxidants from natural sources, regarded as safe alternatives to synthetic products, are important for the food industry because they have fewer potentially adverse side effects [3].

Generally, bioactive peptides (BPs) are inactive within the sequence of the precursor protein molecules but can be released through fermentation, enzymatic or chemical digestion [4]. Proteases could be extracted from plant tissues (e.g., ficin, papain, and bromelain), from animal sources (e.g., trypsin, pepsin, and chymotrypsin) and from microorganisms (e.g., proteinase K, collagenase, subtilisin, alcalase, flavourzyme, and neutrase) [5]. BPs could also be obtained by synthesis chemically or from molecular cloning of appropriate genes. Many BPs exhibit a peptide residue length of 2–20 amino acids [4,6]. BPs may have longer amino acid chains such as proinsulin C-peptide fragments, which are successful for type I diabetes immunotherapy, and plasma C-peptide levels remain a measurement standard for beta cell bioactivity in patients [7]. Furthermore, many bioactive functions of BPs have been systematically reviewed [5,8].

Fish-protein hydrolysates have gained much interest as potential antioxidant BP sources, particularly due to the availability of large quantities of processing by-products and underutilized species [2,3]. It is estimated that fish processing by-products after filleting account for approximately 60–75% of the total fish weight [9,10], and crude protein levels of marine by-products were 8–35% [11]. BPs from marine by-products that are natural and safe alternatives or replacements for synthetic antioxidants seem to be a feasible value-added approach [3,11].

The amino-acid composition, sizes, sequences, and tertiary conformations of the BPs are crucial for their antioxidant activity. The antioxidant BPs are capable of scavenging free radicals, donating electrons and/or chelating metals [3,5]. The potent antioxidant BPs have been shown to contain hydrophobic amino acids (e.g., Pro, Met, Trp and Phe) and one or more residues of His, Cys and Tyr within their sequences [3,12]. Two aromatic amino acids (Tyr and Phe) are known as direct radical scavengers and for special capability of their phenolic groups to serve as hydrogen donors [5]. Cys donates the sulfur hydrogen, and the imidazole group in His has the proton-donation ability for chelating and lipid radical trapping [8]. Hydrophobic amino acids in BPs are particularly important facilitating interaction with lipid for superior radical scavenging activity [3,9,11,13].

The release of BPs from the primary structure of food proteins was achieved by enzymatic hydrolysis with good control of condition parameters as pH, temperature, time, and enzyme/substrate ratio [12]. More recently, ultrasonic-, microwave-, high hydrostatic pressure- and pulsed electric-field-assisted protease hydrolysis was applied to enhance a better production of low molecular weight BPs than the conventional hydrolysis method [14]. In addition to enzymatic hydrolysis, coupling fermentation facilitating improvement of hydrolysis or reduction of bitterness that was commonly produced by extensive hydrolysis is of increasing importance [12,14]. Fractionation and purification of BPs were based on their physicochemical properties, such as molecular weight, net charge, hydrophobicity and hydrophilicity, which were comprehensively reviewed [12]. BP identification (amino-acid sequences) was predominantly conducted by tandem mass spectrometry with protein library/databases or a de novo sequencing approach [12,14]. On the other hand, in silico analysis was a potent alternative approach to reduce the time and labor-consuming experimental work required when discovering new antioxidant peptides [15]. The BIOPEP-UWM (<http://www.uwm.edu.pl/biochemia/index.php/en/biopep>, accessed 3 February 2021) database to unravel the profiles of potential biological activity [16] and a deep convolutional neural network (CNN) classifier, AnOxPePred (<https://services.healthtech.dtu.dk/service.php?AnOxPePred-1.0>, accessed 8 April 2021), to predict antioxidant properties of peptides are the promising strategies [17].

Milk-fat globule membrane (MFGM) is structured when milk-fat globules release into raw milk in the dairy industry [18]. Xanthine oxidase (XOD, EC 1.17.3.2) is one of the most studied enzymes in the MFGM. XOD accounts for about 20% of the total protein

in the MFGM [18]. XOD activity remained in commercial pasteurized milk and induced oxidation of volatile aldehydes and acids, leading to off-flavor and nutritional loss [19].

XOD is a rate-limiting enzyme in the biosynthesis of uric acid that catalyzes the oxidation and breakdown of hypoxanthine to xanthine and subsequently to uric acid [20]. The usage of synthetic drugs such as allopurinol or febuxostat may induce a wide range of side effects, including nausea, diarrhea, arthralgia, headache, increased hepatic serum enzyme levels, and rash [21,22].

Tyrosinase is a copper-containing enzyme that is widely distributed in plants (with particularly high amounts in mushroom, banana, apple, pear, potato, avocado, and peach) [23] and shrimp [24] and is responsible for enzymatic browning of food. Enzymatic browning usually harms the color attribute, sensory properties such as off-flavor, and texture softening. In order to prevent browning, use of food additives has been recognized, including reducing agents and enzyme inhibitors [25]. Hence, enzymatic browning signifies one of the critical problems in the food industry especially for fruits, vegetables, and seafood products. In order to prevent browning, use of food additives has been documented, including reducing agents and enzyme inhibitors. Tyrosinase inhibitors can in principle delay or prevent the browning of fruits, vegetables, and shrimp [26,27].

On the other hand, tyrosinase catalyzes and oxidizes the biosynthesis of the melanin pigment in the melanocytes of human skin. Melanin is responsible for skin color and prevents sun-induced skin damage [28]. When melanin is produced, hydroxyl radicals and other ROS may also be produced [29] leading to the progression of diseases associated with skin injury and cancers [30].

The list of the BPs along with their antioxidant tests can be seen in Table 1. Our previous work showed that HV5 and VW4 peptides, hydrolyzed by papain from mackerel (*Scomber austriasicus*) meat, displayed the extension of induction periods to 6.1 and 7.1 days, respectively, under a lipid peroxide inhibition activity (LPIA) assay [31]. VW4 was further studied for its anti-inflammatory activity using the RAW 264.7 cell model and was found to reduce lipid accumulation, inhibit formation of foam cell induced by ox-LDL, and inhibit gene expression of inducible nitric oxide synthase (iNOS) and scavenger receptor A [32]. PV4 that was hydrolyzed by papain from loach (*Misgurnus anguillicaudatus*) and crude loach protein hydrolysate displayed the ability to scavenge 1,1-diphenyl-2-picrylhydrazyl (DPPH) ( $IC_{50} = 2.64 \pm 0.29$  mg/mL), to scavenge hydroxyl radicals ( $IC_{50} = 17.0 \pm 0.54$  mg/mL), to chelate cupric ion ( $IC_{50} = 2.89 \pm 0.3$  mg/mL), and to inhibit the lipid peroxidation in a linoleic acid emulsion system ( $IC_{50} = 12.3 \pm 0.98$  mg/mL) [33]. NR6 (1 mg/mL from purified BP fraction), which was obtained after in vitro GI tract digestion (pepsin, trypsin, and  $\alpha$ -chymotrypsin) of horse mackerel skin protein, showed high DPPH scavenging activity ( $72.3 \pm 2.5\%$ ) and hydroxyl radical scavenging ability ( $51.2 \pm 2.3\%$ ) [34]. LL4 and PL4 (150  $\mu$ g/mL from purified BP fraction) peptides from *Sardinella aurita* by-products (head and viscera) revealed the ability to scavenge DPPH at  $51 \pm 1.31\%$  and  $52 \pm 1.44\%$ , respectively [35]. LL4 and PL4 were purified from the hydrolysates obtained by treatment from crude enzyme extract from sardine viscera [35]. LY6 peptide obtained from Alaska pollack (*Theragra chalcogramma*) by-product frame protein successfully quenched about 35% of hydroxyl radical [36]. VS14 (1.2 mg/mL from purified BP fraction) from tuna-backbone protein possessed DPPH, hydroxyl, and superoxide radical scavenging ability at about 60%, 80%, and 60%, respectively [37]. VS14 was purified from the pepsin-digested hydrolysates [37]. PV8 that was hydrolyzed and purified from *Ctenopharyngodon idellus* (grass carp) was revealed to have high hydroxyl radical scavenging ability ( $IC_{50} = 2.86 \pm 0.12$  mg/mL) [38]. PV8 was purified from the alcalase digested hydrolysates [38]. LY9 (100  $\mu$ g/mL from purified BP fraction) from the orientase digested *Thunnus tonggol* (tuna) dark meat, a by-product from the canned-tuna processing industry, showed DPPH radical scavenging capacity at  $79.6 \pm 2.86\%$  and the inhibition of lipid oxidation [39]. Moreover, IW3, a potent ACE inhibitor, obtained from thermolysin-pepsin hydrolysate of ovotransferrin from egg white, was selected as a positive control in this study [40]. IW3 showed anti-inflammatory and antioxidant activities on human

endothelial cells by decreasing the cytokine-induced inflammatory protein expression. The well-known bioactive tri-peptide exhibited multifunction as inhibiting inflammatory and oxidative stress [41], against angiotensin II stimulation [42], and improving impaired insulin sensitivity by down-regulating the activation of p38 and JNK1/2 in TNF- $\alpha$ -treated skeletal muscle cells [43]. In the animal models, IRW can mitigate dextran sodium sulfate-induced oxidative stress by increasing intestinal microbiota abundance and maintaining homeostasis of host health [44], regulate *Citrobacter rodentium*-induced colonic inflammation, and improve intestinal microbial and metabolomics levels [45], and reduce blood pressure in spontaneously hypertensive rats [46].

**Table 1.** Antioxidant activity and the original source of the bioactive peptides.

Peptide Sequence	Source (By-Product)	Enzyme	Antioxidant Activity	Reference
HV5 (HGAYV, 380 Da)	Mackerel meat ( <i>Scomber austriasicus</i> )	Papain	LPIA	[31]
VW4 (VWWW, 680 Da)	Mackerel meat ( <i>Scomber austriasicus</i> )	Papain	LPIA, cell model	[31,32]
IW3 (IRW, 340 Da)	Egg white	Thermolysin, pepsin	Cell model	[40]
PV4 (PSYV, 464.2 Da)	Loach meat ( <i>Misgurnus anguillicaudatus</i> )	Papain	HRSA, DPPH, Cu <sup>2+</sup> ion, LPIA	[33]
NR6 (NHRYDR, 856 Da)	Horse mackerel (skin) ( <i>Magalaspis cordyla</i> )	In vitro-GI tract digestion	RP, Chelating activity, DPPH, HRSA	[34]
LL4 (LARL, 471.3 Da)	Sardinelle (head and viscera) ( <i>Sardinella aurita</i> )	Crude enzymes from viscera of sardine	DPPH, LPIA, RP	[35]
PL4 (PHYL, 528.2 Da)	Sardinelle (head and viscera) ( <i>Sardinella aurita</i> )	Crude enzymes from viscera of sardine	DPPH, LPIA, RP	[35]
LY6 (LPHSGY, 672 Da)	Alaska pollack (frame protein) ( <i>Theragra chalcogramma</i> )	Mackerel intestine crude enzyme	LPIA, HRSA	[36]
VS14 (VKAGFAW TANQQLS, 1519 Da)	Tuna (backbone protein)	Pepsin	DPPH, HRSA, superoxide, LPIA	[37]
PV8 (PSKYEPFV, 966.3 Da)	Grass carp meat ( <i>Ctenopharyngodon idellus</i> )	Alcalase	HRSA, LPIA	[38]
LY9 (LPTSEAAKY, 978 Da)	Tuna (dark meat) ( <i>Thunnus tonggol</i> )	Orientase	DPPH, LPIA	[39]

HRSA: Hydroxyl Radical Scavenging Activity; LPIA: Lipid Peroxide Inhibition Activity; RP: Reducing Power.

This study first applied the commonly used in vitro antioxidant assays, including DPPH, trolox equivalent antioxidant capacity (TEAC) and reducing powder (RP), to compare the antioxidant activity of the selected 11 BPs. In silico analysis was performed using the BIOPEP-UWM database, and an AnOxPePred algorithm was used to predict and evaluate antioxidant properties of BPs. The potent antioxidant BPs were elaborated in their antioxidant capacities to XOD inhibition for preventing milk fat oxidation and anti-browning for inhibiting food-derived tyrosinase oxidation. The kinetic activities of the potential BPs against XOD and tyrosinase were also analyzed.

## 2. Materials and Methods

### 2.1. Chemicals

The 11 BP samples were synthesized by TOOLS Biotechnology Co., Ltd. (New Taipei City, Taiwan), and certificates of analysis were at the highest purity (>95%) by using high-performance liquid chromatography. The BPs were HV5 (HGAYV, mackerel), VW4 (VWWW, mackerel), IW3 (IRW, egg white), PV4 (PSYV, loach), NR6 (NHRYDR, horse mackerel), LL4 (LARL, sardinella), PL4 (PHYL, sardinella), LY6 (LPHSGY, Alaska pollock), VKAGFAWTAN-QQLS (VS14, tuna), PSKYEPFV (PV8, grass carp) and LY9 (LPTSEAAKY, tuna). Potassium ferricyanide ( $K_3Fe(CN)_6$ ), ferric chloride ( $FeCl_3$ ), and trichloroacetic acid (TCA) were purchased from Riedel-de Haën (Darmstadt, Germany). Hydrochloric acid (HCl), ascorbic acid, monosodium phosphate ( $NaH_2PO_4$ ), and disodium phosphate ( $Na_2HPO_4$ ) were purchased from Merck (Darmstadt, Germany). Ethanol, 2,2'-azino-bis(3-ethylbenzothiazoline-6-sulfonic acid) diammonium salt (ABTS), 1,1-diphenyl-2-picrylhydrazyl (DPPH), 6-hydroxy-2,5,7,8-tetramethylchromane-2-carboxylic acid (Trolox), potassium persulfate ( $K_2S_2O_8$ ), xanthine oxidase (EC number: 1.17.3.2), xanthine, allopurinol, tyrosinase (EC 1.14.18.1), and L-tyrosine were purchased from Sigma-Aldrich (St. Louis, MO, USA).

### 2.2. DPPH Assay

The DPPH assay was performed on the basis of a method [47]. An aliquot of 150  $\mu$ L of the BPs (5 mg/mL in distilled water) was mixed with 200  $\mu$ L of methanol solution containing 1 mM DPPH radicals. The mixture was incubated for 30 min in the dark, and absorbance was monitored at 517 nm using the Multiskan GO Microplate Spectrophotometer 51119300 (Thermo Fisher Scientific Inc., Waltham, MA, USA). The absorbance decrease at 517 nm between the blank and a sample was used for calculating scavenging activity. The percentage of decrease was determined according to the amount of discoloration. The ascorbic acid at 1 mg/mL was used as a positive control. Each experiment was performed in triplicate.

### 2.3. ABTS Assay

The trolox equivalent antioxidant capacity (TEAC) assay was performed on the basis of the method [48]. A 100  $\mu$ L sample solution (0.25 mg/mL) was mixed with 1 mL of the ABTS radical solution (30 mL of ABTS at 10 mM and 15 mL of  $K_2S_2O_8$  at 8.17 mM, with 16 h incubation at 40 °C). The ABTS radicals were diluted prior to use with a 0.01 M phosphate buffer at pH 7.4 until the absorbance of the solution at 734 nm reached  $0.8 \pm 0.02$ . The sample and ABTS radical mixture were incubated for 6 min in the dark, and the absorbance was monitored at 734 nm using a Multiskan GO Microplate Spectrophotometer 51119300 (Thermo Fisher Scientific Inc., Waltham, MA, USA). The absorbance decrease at 734 nm between the blank and a sample was used to calculate scavenging activity. Trolox was prepared as a standard curve to achieve the TEAC. Results are presented as the means of experiments performed in triplicate  $\pm$  standard deviation.

### 2.4. Reducing Power Assay

The reducing power (RP) assay was performed on the basis of the method [49], in which 100  $\mu$ L of each sample (5 mg/mL) was added to 100  $\mu$ L of 0.2 M phosphate buffer (pH 6.6) and 100  $\mu$ L of 1% potassium ferricyanide. The mixtures were incubated at 50 °C for 20 min, and then 100  $\mu$ L of 10% trichloroacetic acid was added to each reaction mixture. Next, 100  $\mu$ L from each incubated mixture was mixed with 100  $\mu$ L of distilled water and 20  $\mu$ L of 0.1% ferric chloride in tubes. After 10 min, the solutions were measured at 700 nm using the Multiskan GO Microplate Spectrophotometer 51119300 (Thermo Fisher Scientific Inc., Waltham, MA, USA). Increased absorbance of the reaction mixture indicated increased RP. The ascorbic acid was prepared as a standard curve to achieve ascorbic acid equivalent antioxidant capacity (AEAC). Each experiment was performed in triplicate.

### 2.5. *In Silico* Analysis of 11 Bioactive Peptides (BPs)

The selected 11 BPs were further investigated by using the BIOPEP-UWM (<http://www.uwm.edu.pl/biochemia/index.php/en/biopep>, accessed 3 February 2021) database. BPs were individually analyzed by BIOPEP-UWM tools to unravel the profiles of potential biological activity [16]. The 11 BPs were also put in a deep convolutional neural network (CNN) classifier, AnOxPePred (<https://services.healthtech.dtu.dk/service.php?AnOxPePred-1.0>, accessed 8 April 2021), for predicting antioxidant activity, including free radical scavenging (FRS) and metal chelating activity (MCA) scores, with its predictions being from 0 (not antioxidant) to 1 (antioxidant) [17].

### 2.6. XOD Inhibition Assay

XOD activity with xanthine as the substrate was measured spectrophotometrically using the method [50], in which peptide samples (1 mg/mL) were mixed with 0.05 M phosphate buffer (pH 7.5) and 0.5 units/mL XOD solution. After 10 min of incubation at room temperature (27 °C), xanthine substrate solution at several concentrations (1.5, 3.0, 5.0, 6.0 and 10.0 M) was added to this mixture. The mixture was again incubated for 30 min at room temperature (27 °C), and the absorbance was measured every minute at 293 nm by using the Multiskan GO Microplate Spectrophotometer 51119300 against blank and a positive control (Allopurinol at the final concentration 0.1 mg/mL). The half-maximal inhibitory concentration (IC<sub>50</sub>) was determined after 20 min of incubation. Each experiment was performed in triplicate.

The kinetic parameters were obtained using the Michaelis-Menten equation and Lineweaver-Burk plots that were plotted and derived using SigmaPlot 12.5 (SigmaPlot Software Inc., San Jose, CA, USA).

### 2.7. Tyrosinase Inhibition Assay

Tyrosinase inhibitory activity was measured according to the method [51], in which peptide samples (0.5 mg/mL) were mixed with 30 mM sodium phosphate buffer (pH 6.8) and 0.5 mg/mL tyrosinase solution. After 5 min of incubation at 37 °C, L-tyrosine solution at several concentrations (0.5, 1.0, 1.5 and 2.0 mM) was added. This mixture was incubated at 37 °C for 20 min, and the absorbance was measured at 475 nm every minute using the Multiskan GO Microplate Spectrophotometer 51119300. The control represented the absorbance of the solution without the test sample and the presence of the enzyme after incubation. Blanks represented the absorbance of the solution with the test sample and the absence of the enzyme after incubation. Each experiment was performed in triplicate.

Kinetic parameters were obtained using the Michaelis-Menten equation and Lineweaver-Burk plots that were plotted and derived using SigmaPlot 12.5 (SigmaPlot Software Inc., San Jose, CA, USA).

### 2.8. Statistical Analysis

Statistical analysis was performed using one-way ANOVA with SPSS 20 (IBM Corp., Armonk, USA). Mean values for the treatments were compared using Duncan's multiple-comparison tests  $p < 0.05$ .

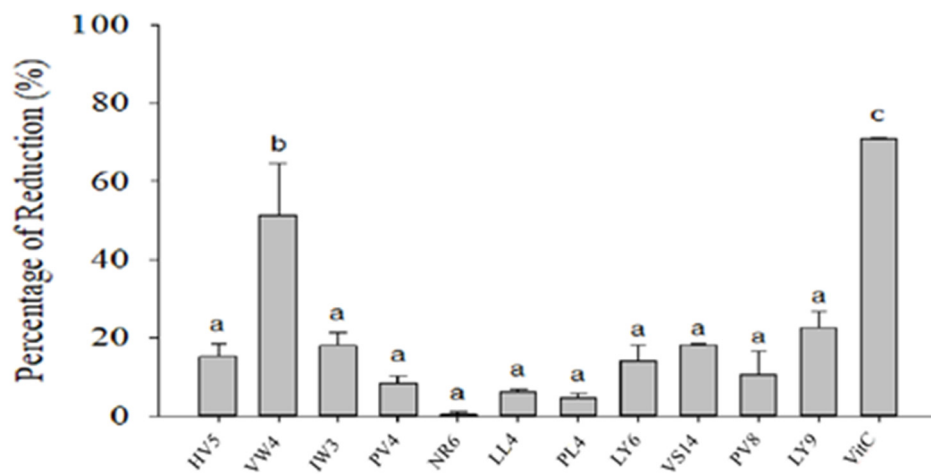
## 3. Results and Discussion

### 3.1. Antioxidant Activities of 11 Selected BPs

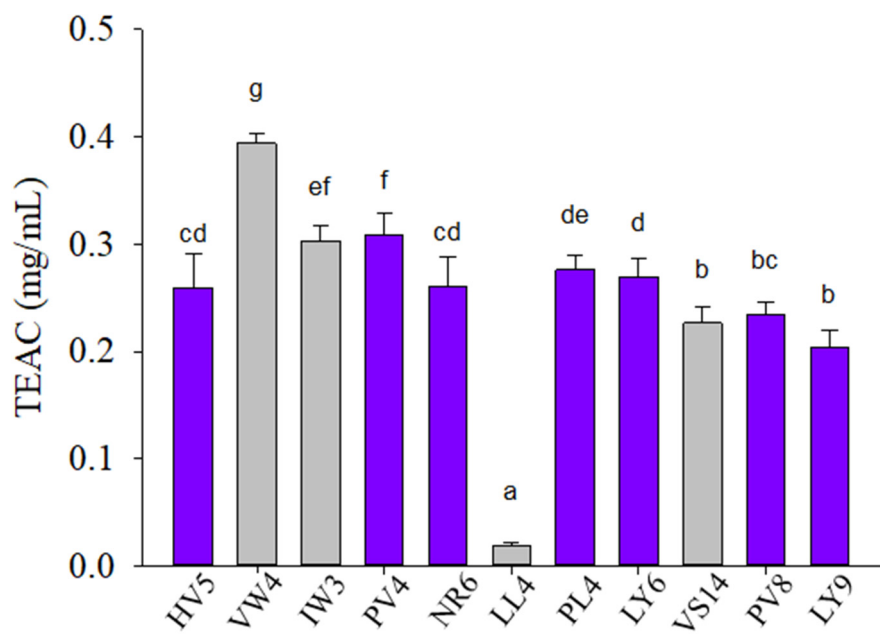
Several known sources of BPs from marine protein hydrolysates with potential antioxidant activity were selected for this study. The selection criteria were enzymatically digested oligopeptides from bulky catch species in China as freshwater farmed loach [33] and grass carp meat hydrolysates [38], and in Taiwan as wild-capture mackerel meat hydrolysates from our previous work [31,32]. The other sources were the by-products (e.g., head, viscera, skin, frame and dark meat) of bulky capture species as shown in Table 1. These BPs derived from fish species included mackerel (*Scomber austriasicus*) [31,32], loach (*Misgurnus anguillicaudatus*) [33], horse mackerel (*Magalaspis cordyla*) [34], sardinella (*Sardinella aurita*) [35],

Alaska pollock (*Theragra chalcogramma*) [36], tuna (*Thunnus tonggol*) [37,39], and grass carp (*Ctenopharyngodon idellus*) [38]. Moreover, 9 out of the 11 selected BPs were conducted for the inhibition on autoxidation of linoleic acid (also called lipid peroxide inhibition activity, LPIA), mimicking protection from high lipid food deterioration (Table 1). The well-known multifunctional bioactive tri-peptide (IW3) derived from egg white-ovotransferrin was selected as a positive control [40].

As a stable radical, DPPH is widely used to determine the antioxidant activity of active compounds. The DPPH assay result is presented in Figure 1a. In this DPPH assay, the ascorbic acid was used as a positive control at a concentration of 1 mg/mL. The concentration of the BPs was 5 mg/mL. Peptide samples could reduce DPPH by a range of 0.41–51.29%, and the highest antioxidative capacity was observed to be in VW4, followed by LY9, IW3, and VS14, whereas the lowest antioxidant activity was exhibited by NR6. The positive control demonstrated 70.73% reduction ability against DPPH. However, NR6 revealed high DPPH scavenging activity ( $72.3 \pm 2.5\%$ ) at 1 mg/mL by electron spin resonance (ESR) spectroscopy [34]. This inconsistency may be caused by different treatment doses (1 and 5 mg/mL), different assays (ESR spectroscopy and colorimetry), and different sources (purified digested peptides and synthesized peptides) [34]. More recently, antioxidant BPs from Alcalase-treated gelatin hydrolysates of seabass skin were separated using Sephadex G-25 then reverse phase-high performance liquid chromatography (RP-HPLC), and subsequently identified using UPLC-ESI-MS/MS [52]. A total of 48 peptides were identified from 2 fractions (fraction 12 and 16) with the highest ABTS radical scavenging activity, separated by RP-HPLC. Four selected BPs from the 48 identified BPs, containing Gly-Pro-X motif and with the highest average local confidence (ALC), were further synthesized and showed varying ABTS radical-scavenging activity (0.50–81.41 mMol Trolox equivalent/ $\mu\text{mol}$  peptide). Low ABTS radical-scavenging activity (0.50 mMol Trolox equivalent/ $\mu\text{mol}$  peptide) of Gln-Leu-Gly-Pro-Leu-Gly-Pro-Val was assumed to be the improper conformation of the peptide for quenching ABTS radicals [52]. It indicated a big contradiction of bioactivity between purified hydrolysates and synthesized BPs. The high DPPH scavenging activity that was observed from a hydrolysate fraction of horse mackerel skin [34] might have originated from other peptides than NR6. The protein source, degree of hydrolysis, amino acid composition, molecular weight, and peptide sequences have been suggested to determine the bioactivity and functional properties of BPs [2,3,5,6,8,10]. The antioxidant activity of BPs has been suggested to derive from amino acids present in the sequence, particularly from Trp, Met, Cys, Tyr, Phe, and His [33–35,53]. Hydrophobic amino acids with nonpolar aliphatic chain and aromatic groups (Leu, Trp, Tyr, Phe, Ile, Val) effectively scavenge free radicals in high lipid food [8,31,32,35,54]. VW4 (VWWW) and IW3 (IRW) had both hydrophobic aliphatic chain and aromatic groups, and IW3 also contained one positively charged residue. VS14 (VKAGFAWTANQQLS) completely fulfilled the rule that hydrophobic amino acids, charged residues and one of more residues of His, Pro, Met, Cys, Trp, Phe and Tyr were within their sequences [3,12,13]. VS14 (1.2 mg/mL from purified BP fraction) from tuna-backbone protein showed good DPPH radical-scavenging ability at about 60% [37]. LY9 (LPTSEAAKY) agreed with BPs from soybean hydrolysates that had shown potent radical scavenging activity due to Val or Leu at the N-terminal position as well as Pro, His or Tyr in the sequence [11,39,55]. LY9 (100  $\mu\text{g}/\text{mL}$  from purified BP fraction) from the orientase digested *Thunnus tonggol* (tuna) dark meat showed DPPH radical-scavenging capacity at  $79.6 \pm 2.86\%$  [39]. Hence, VW4, LY9, IW3 and VS14 were selected as potential BPs for the further XOD and tyrosinase inhibition assay according to the greater DPPH radical-scavenging activity.



(a)



(b)

Figure 1. Cont.

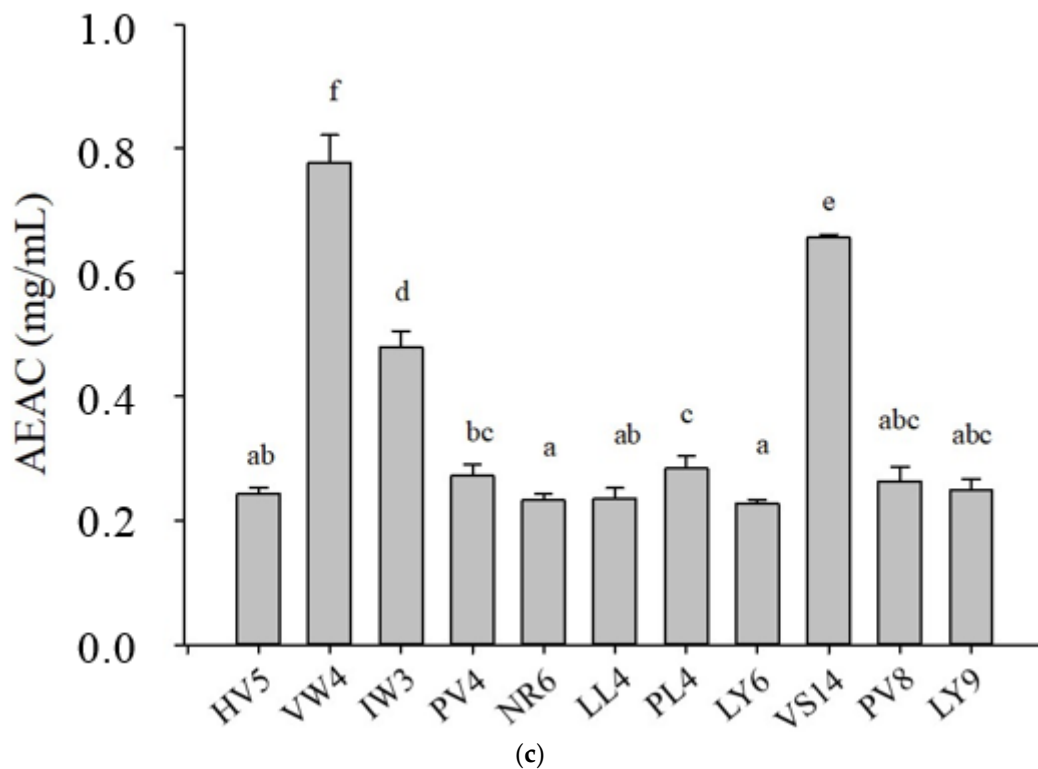


**Figure 1.** In vitro antioxidant assay of BPs. (a) DPPH assay of BPs. Results are expressed as the percentage reduction ability of the BPs at 5 mg/mL and ascorbic acid at 1 mg/mL. (b) ABTS assay of BPs. The concentration of BPs is 0.25 mg/mL. Results are expressed for Trolox equivalent antioxidant capacity (TEAC) in mg/mL. (c) RP assay of BPs. The concentration of BPs was 5 mg/mL. Results are expressed for ascorbic acid equivalent antioxidant capacity (AEAC) in mg/mL. Data are expressed as means  $\pm$  SD of triplicates. Letters denote significant difference ( $p < 0.05$ ).

The results of the ABTS assay are presented in Figure 1b. The concentration of the BPs in the assay was 0.25 mg/mL. At that concentration, the peptide samples exhibited antioxidant capacities equivalent to those of Trolox (TEAC) at a range (0.019–0.394 mg/mL). VW4 exhibited the highest antioxidant activity followed by PV4 and IW3. The other peptides revealed considerable degrees of antioxidant activity, except for LL4. The ABTS assay partially confirmed the DPPH result that VW4 and IW3 revealed the superior radical-scavenging activity. The ABTS assay for all test BPs displayed two types of color changes. Common antioxidants as BPs without Tyr residue, phenolics and flavonoids in ABTS assay discolored the ABTS radical from bluish green to colorless ABTS. However, several peptides, namely HV5, PV4, NR6, PL4, LY6, PV8, and LY9, changed the color of the ABTS radical, not to colorless but to purplish blue. This may be attributable to the presence of Tyr in the peptide sequence. Tyr can bond covalently with the ABTS radical to generate purple adduct [36]. A novel peptide ATVY from black shark-skin protein hydrolysates showed high ABTS scavenging activity, and the key action site was demonstrated as the crucial amino acid in the N-terminal position (Tyr) [56]. ATVY reacted with ABTS to generate polyphenol-derived adducts that subsequently degraded into a purple compound, which was developed by covalently bonding through the phenol group of ATVY to the N group of ABTS [56]. The purple compounds were not investigated in this study. We encourage future study to test ABTS scavenging activities of Tyr-containing peptides.

Figure 1c illustrates the results of RP for BPs, which were used at 5 mg/mL. BPs possessed antioxidant capacity relative to ascorbic acid (AEAC) at a range of 0.227–0.777 mg/mL. The highest relative absorbance was in VW4, followed by VS14 and IW3. The RP assay partially confirmed the DPPH result that VW4, VS14 and IW3 revealed the superior antioxidant activity. Because a reducing compound could donate an electron to a free radical, radicals could be neutralized and the reduced species could

acquire a proton from the solution. Thus, reducing capable compounds could also have fostered antioxidative ability [57]. Studies have reported that Leu, Lys, Met, Ile, and His are related to strong RP [58,59], and aromatic amino acids (Trp, Tyr, Phe) may promote chelating pro-oxidants [5,13,33,34]. Several amino acids, particularly His, Glu, and Asp, could chelate transition metals [54]. The reducing capable amino acids are more abundant and possibly constituting suitable conformations in VW4, VS14 and IW3, contributing to their greater RP than other test BPs.

In summary, VW4, IW3 and VS14 were selected to the enzyme inhibition assay according to their superior antioxidant activity based on DPPH, RP and ABST results.

### 3.2. In Silico Analysis of Biological Activities of 11 Selected BPs

In silico analysis of biological activities of the BPs was performed using the BIOPEP-UWM database [16]. Briefly, the bioactivities and sequences were analyzed using the “profiles of potential bioactivity” tool. As shown in Table 2, most BPs contained potential antioxidant peptide fragments except sample PV4 and NR6. Six of the 11 BPs (IW3, LL4, PL4, LY6, PV8 and LY9) have information regarding antioxidant activity of the full peptide sequences. In addition, all BP fragments showed potential ACE and DPP IV inhibitory activities. IW3 not only proposes to have the most versatile application for different kinds of bioactive functions but also correlated to in vitro antioxidant assay and demonstrated good XOD inhibition due to the abundant academic publications [40–46]. VW4 may also be an inhibitor for  $\alpha$ -glucosidase. With appropriate enzymatic digestion, these bioactive peptides with different biological activities can be released and further studied in in vitro or in vivo tests.

**Table 2.** List of activities of peptides annotated in the BIOPEP-UWM database, and antioxidant activity prediction by AnOxPePred algorithm for the test bioactive peptides.

Sample	ACE Inhibitory	DPP IV Inhibitor	Antioxidant	Others	FRS Score	MCA Score
HV5	AY, GA, HG, YV	AY, GA, YV	AY	-	0.52	0.24
VW4	VW	WWW, WW, VW	VW	VW (Alpha-glucosidase inhibitor)	0.62	0.20
IW3	IRW, RW, IR	RW, IR	IRW, RW, IR	IRW (hypotensive, anti-inflammatory), RW (DPP-III inhibitor), IR (Renin inhibitor, CaMPDE inhibitor)	0.43	0.22
PV4	PSY, SY, YV	PS, SY, YV	-	-	0.45	0.23
NR6	RY	DR, HR, NH, YD	-	-	0.48	0.19
LL4	RL, LA, AR	LA, RL	LARL	LA (DPP-III inhibitor, activating ubiquitin-mediated proteolysis)	0.36	0.24
PL4	HY, PH	HY, PH, YL	PHY, PHYL	YL (neuropeptide), HY (anti-inflammatory), YL (DPP-III inhibitor)	0.57	0.28
LY6	GY, SG, PH	LP, GY, HS	LPHSGY, PHS	PH (DPP-III inhibitor)	0.52	0.29
VS14	AW, VK, KA	KA, FA, TA, WT, AW, NQ, QL, QQ, VK	AW	KA, FA (DPP-III inhibitor)	0.51	0.24

Table 2. Cont.

Sample	ACE Inhibitory	DPP IV Inhibitor	Antioxidant	Others	FRS Score	MCA Score
PV8	KY, YE	EP, KY, PF, PS, SK, YE	PSKYEPFV	PF (DPP-III inhibitor)	0.51	0.19
LY9	AA, EA, KY, PT	LP, AA, KY, PT, TS	LPTSEAAKY	SE (stimulating), LPTSEAAKY (anticancer), EA (alpha-glucosidase inhibitor)	0.35	0.24

ACE: Angiotensin-converting-enzyme; DPP: Dipeptidyl peptidase IV inhibitor; CaMPDE: Calmodulin-dependent cyclic nucleotide phosphodiesterase; FRS: Free radical scavenging; MCA: Metal chelating activity.

Another prediction neural network algorithm was recently developed as AnOxPePred, and it will provide a probability score of the peptide being either a free radical-scavenging (FRS) or metal-chelating activity (MCA) [17]. As shown in Table 2, BPs received a range of 0.35–0.62 FRS scores. FRS confirmed all antioxidant assays, including DPPH, ABTS and RP results that VW4 revealed the best antioxidant activity. But LY9 and LL4 received the lowest scores of FRS and less than 0.40. However, LY9 showed the second DPPH scavenging activity among 11 test BPs. BPs had a range of MCA scores (0.19–0.29). LY6 showed the highest level, but NR6 and PV8 received the lowest levels. It was evident that His is inherently more present in antioxidant BPs (1st MCA and 3rd FRS rankings), followed by Trp (1st FRS), Tyr (2nd FRS), and Pro (2nd MCA), according to the differential analysis between the antioxidant dataset and a baseline from UniProtKB/Swiss-Prot databank [17]. Therefore, VW4 (VWWW) received the first place of FRS. AnOxPePred has achieved a promising deep-learning prediction of antioxidant peptides based solely on their sequences. The algorithm can considerably improve its accuracy and usefulness while the peptide structure, hydrophobicity, and solubility are included in the model in the future [15,17].

### 3.3. XOD Inhibitory Activity of Selected BPs

The Lineweaver-Burk plot for XOD inhibition is presented in Figure 2. This plot describes the velocity of the XOD reaction in the presence and/or absence of inhibitors. Control represented reaction velocity in the absence of inhibitors (control). Allopurinol was used as a positive control. Higher concentration of the substrate (xanthine) corresponded to faster reaction velocity. In general, the speed of uric-acid formation was highest after the substrate reached 5.0 mM (plateau). Uric-acid formation speed was the lowest when allopurinol was involved in the reaction. In addition, VS14, IW3, and VW4 displayed slower uric-acid formation than the negative control. These results indicate that allopurinol could inhibit XOD most effectively, followed by VS14, IW3, and VW4. Vmax and Km values of the samples are listed in Table 3.

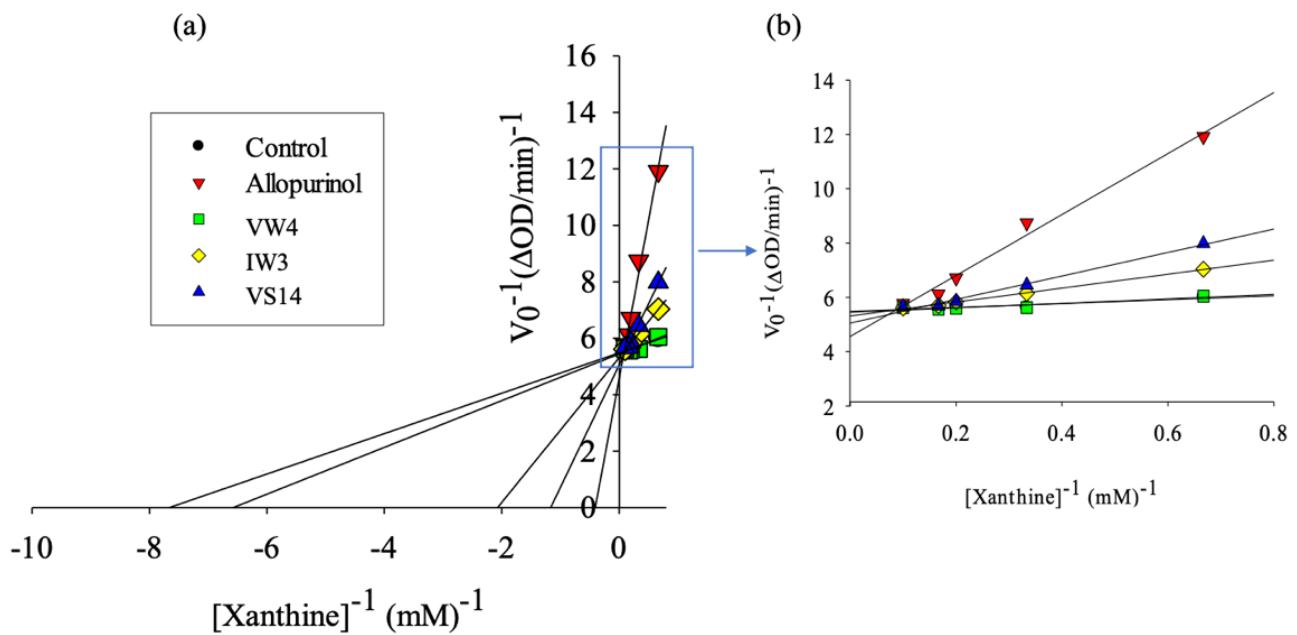


**Figure 2.** (a) Lineweaver-Burk model of VW4, IW3 and VS14 against allopurinol as the positive control for XOD inhibition assay. The concentration of peptide used was 1 mg/mL, while concentration of allopurinol was 0.1 mg/mL. (b) The plot in the squared area (from 0.0  $mM^{-1}$  to 1.0  $mM^{-1}$  xanthine) is displayed at a higher magnification.

**Table 3.**  $IC_{50}$ ,  $V_{max}$ , and  $K_m$  value of the bioactive peptides in the inhibition of xanthine oxidase.

Sample	$IC_{50}$ (mg/mL) *	$IC_{50}$ (mM)	$V_{max}$ ( $\Delta OD/min$ )	$K_m$ (mM)
Control			0.182	0.127
Allopurinol	$0.171 \pm 0.001$ <sup>a,+</sup>	$1.253 \times 10^{-3}$	0.223	2.544
VW4	$3.611 \pm 0.105$ <sup>d</sup>	5.310	0.183	0.147
IW3	$1.338 \pm 0.015$ <sup>b</sup>	3.935	0.188	0.478
VS14	$2.740 \pm 0.022$ <sup>c</sup>	1.804	0.196	0.816

<sup>+</sup> Value is expressed in  $\mu g/mL$ . \* Expressed as means  $\pm$  SD of triplicates. Values in the same column followed by different letters are significantly different ( $p < 0.05$ ).

The  $IC_{50}$  values (mM) in Table 3 indicate that the BP with the highest inhibition capability was VS14, followed by IW3 and VW4. IW3 showed the lowest  $IC_{50}$  value ( $1.338 \pm 0.015$  mg/mL), and that 4-fold molecular weight difference between IW3 and VS14 caused this inconsistency. A study performed on several amino acids and dipeptides concluded that Trp induced XOD inhibitory activity [60]. A recent study indicated that WPPKN and ADIYTE from walnut-protein-derived peptides were shown to be potential XOD inhibitors in hyperuricemia rats [61]. The  $IC_{50}$  values of tetra- and penta-peptides from walnuts showed a significant difference by the presence or absence of Trp, and it indicated that VPPW were significantly superior to VWPP [62]. Trp residues were proved to promote XOD inhibition and antioxidant activities via evaluating 20 amino acids, 400 dipeptides and 8000 tripeptides by Autodock Vina molecular docking analysis. The Trp residue ranked the top Vina score among 20 amino acids. Trp also achieved the highest Vina score followed by Arg and Phe regarding tripeptides. The number of amino acid and Trp positions had a certain effect on XOD inhibition and antioxidant activities of Trp-containing peptides [62]. One possible explanation for this phenomena was that Trp has an indo ring, a structure analogous with allopurinol [62]. These lines of evidence support VS14, VW4 and IW3 being potent XOD inhibitors, especially for the presence of Trp and its numbers and positions. XOD in the milk-fat globule membrane (MFGM) could oxidize the abundant flavor aldehydes such as acetaldehyde, hexanal, propanal,

trans-2-nonenal, trans-2-heptenal, and trans-2-hexenal, leading to oxidative deterioration and off-flavor of milk [63]. Commercial pasteurization (70 °C or 75 °C for 15 s) cannot inhibit XOD activity but increases its activity. On the other hand, UHT can avoid XOD oxidation. The residual XOD activity in pasteurized whole milk could be retained more than UHT whole milk after in vitro digestion, resulting in an increase of uric-acid level in vitro and in vivo [64]. The VW4, IW3 and VS14 are the promising XOD inhibitors for the pasteurized whole milk. Regarding caffeic acid roasting products, the roasting temperature significantly affects XOD inhibitory activities. Caffeic acid and its coupling product (vinylcatechol), largely produced at 140–170 °C, revealed stronger XOD inhibition than the other types of oligomers produced [65]. The  $IC_{50}$  values of BPs and allopurinol were not at the same order of magnitude found in this study that was in agreement with a novel XOD inhibitory peptide (ACECD) purified from Skipjack tuna [66], and FDAK from Pacific Bluefin tuna [60]. The  $IC_{50}$  value of ACECD was 7.23 mg/mL, but that of allopurinol was much lower at 8.04  $\mu\text{g/mL}$  [66]. Computer-aided molecular docking showed ACECD inserted into the active site of XOD via a competitive binding mode [66]. Several BPs with XOD inhibitory activity had  $IC_{50}$  values from 0.95 to 25.7 mM [67]. Table 3 shows  $IC_{50}$  for VW4, IW3, and VS14 were 5.310, 3.935 and 1.804 mM, respectively. Due to the lower range of the specified interval, VW4, IW3, and VS14 are promising XOD inhibitors to protect milk-fat oxidation in the dairy industry.

### 3.4. Tyrosinase Inhibitory Activity of Selected BPs

Figure 3 displays the Lineweaver-Burk plot of tyrosinase inhibition, demonstrating similar tyrosinase inhibitory activity among VW4, VS14, and IW3. Calculating  $V_{\text{max}}$  and  $K_{\text{m}}$  values in the tyrosinase inhibition assay revealed the competitive inhibition pattern for all BPs, as characterized by the same value of  $V_{\text{max}}$  and increasing value of  $K_{\text{m}}$  in Table 4. The  $IC_{50}$  of each peptide is presented in Table 4. The  $IC_{50}$  calculation revealed that IW3 had the lowest inhibition ability against tyrosinase, signified by the high value of  $IC_{50}$ . The highest inhibition capability was displayed by VS14 at 0.595 mM, followed by VW4 and IW3. But VW4 showed the lowest  $IC_{50}$  value by mg/mL, and this inconsistency may be caused by a 2-fold molecular weight difference between VW4 and VS14.

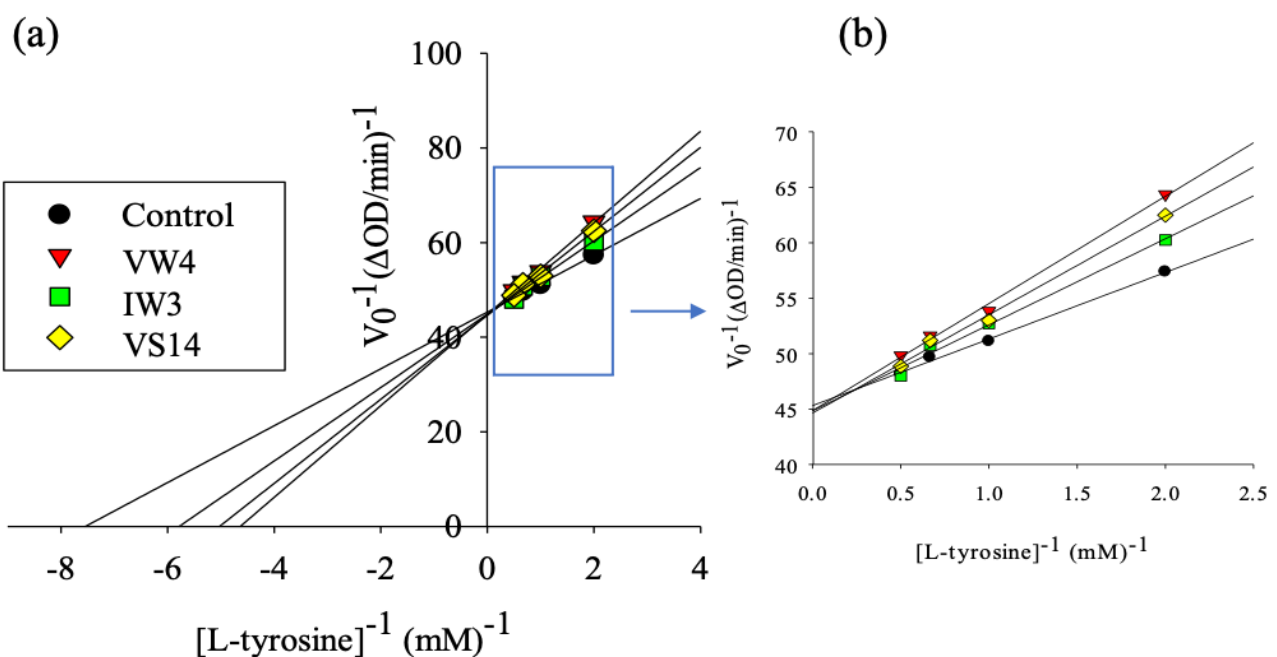


**Figure 3.** (a) Lineweaver-Burk model of peptides VW4, IW3, and VS14 against the control for the tyrosinase inhibition assay. The concentration of peptide used was 0.5 mg/mL. (b) The plot in the squared area (from 0.0  $\text{mM}^{-1}$  to 2.0  $\text{mM}^{-1}$  L-tyrosine) is displayed at a higher magnification.

**Table 4.** IC<sub>50</sub>, V<sub>max</sub>, and K<sub>m</sub> value of the bioactive peptides in the inhibition of tyrosinase.

Sample	IC <sub>50</sub> (mg/mL) *	IC <sub>50</sub> (mM)	V <sub>max</sub> (ΔOD/min)	K <sub>m</sub> (mM)
Control			0.022	0.132
VW4	0.853 ± 0.027 <sup>a</sup>	1.254	0.022	0.212
IW3	0.984 ± 0.009 <sup>c</sup>	2.895	0.022	0.176
VS14	0.903 ± 0.009 <sup>b</sup>	0.595	0.022	0.198

\* Expressed as means ± SD of triplicates. Values in the same column followed by different letters are significantly different ( $p < 0.05$ ).

The individual Michaelis-Menten plot and Lineweaver-Burk plot of the VW4, IW3, and VS14 are available in the supplementary data. Peptides may have the ability to reduce o-dopaquinone to DOPA as a result of dopachrome and melanin formations being avoided [68]. Other than the mechanisms for reducing o-dopaquinone, there are also several mechanisms of tyrosinase inhibition including those involving o-dopaquinone scavenger (thiol compounds), nonspecific enzyme inactivators (acids or bases), and alternative enzyme substrates such as several phenolic compounds (XOD transforms phenolic compounds into quinones) [68]. Tyrosinase is responsible for enzymatic browning, particularly in shrimp and plant food during handling, storage, and processing under oxygen-exposure conditions. The browning effect on food leads to a substantial loss of nutritional quality, color, consumer demand, and commercial value [27]. Naturally occurring flavonoids are the most prominent tyrosinase inhibitors. Moreover, many synthetic tyrosinase inhibitors have already been reported with the IC<sub>50</sub> values even less than 1 μM [25]. The structure-activity relationship of these potent tyrosinase inhibitors, primarily from plants and recently from microorganisms, has also been comprehensively reviewed [69]. The VS14, VW4, and IW3 showed their potential anti-browning capacity for protection from enzymatic browning of food, although they still cannot compete with phytochemicals such as phenols and flavanones [69]. However, the IC<sub>50</sub> values may be incomparable due to the different assay conditions (different substrate concentrations, incubation time, and different sources of tyrosinase) [69]. Tyrosinase inhibitory activity may still be a desirable attribute in protein hydrolysates from marine by-products.

#### 4. Conclusions

This study revealed that VW4 possessed the highest in vitro antioxidant activity based on DPPH, TEAC, RP results and FRS score from the AnOxPePred algorithm. VS14, IW3, and VW4 exhibited superior XOD inhibitory activity due to their lower IC<sub>50</sub> levels when comparing other natural sources, although they still cannot compete with allopurinol [60]. However, concerning food safety and the nature of BPs, they are more suitable than allopurinol for the food industry. Furthermore, the potent XOD inhibitory activity of BPs could prevent oxidative off-flavor formation in pasteurized whole milk due to residual XOD activity. VS14 also revealed the highest inhibition ability of tyrosinase among the BPs. Overall, VW4, IW3, and VS14 have great potential of being safe and natural antioxidants, for anti-enzymatic browning, and as anti-XOD agents.

**Supplementary Materials:** The following are available online at <https://www.mdpi.com/article/10.3390/pr9050747/s1>, Figure S1: Michaelis-Menten model of chosen bioactive peptides; i.e., VW4 (VWWW, Peptide 2), IW3 (IRW, Peptide 3), and VS14 (VKAGFAWTANQQLS, Peptide 9); against allopurinol as positive control and control for xanthine oxidase inhibition assay. The concentration of peptide used was 1 mg/mL, while concentration of allopurinol was 0.1 mg/mL. Data expressed as means ± SD of triplicates. Figure S2: (a) Lineweaver-Burk model of allopurinol as positive control against control for xanthine oxidase inhibition assay. (b) The plot in squared area (from 0.0 mM<sup>-1</sup>–1.0 mM<sup>-1</sup> Xanthine) is exhibited at higher magnification. Figure S3: (a) Lineweaver-Burk model of VW4 against control for xanthine oxidase inhibition assay. (b) The plot in squared area (from 0.0 mM<sup>-1</sup>–1.0 mM<sup>-1</sup> Xanthine) is exhibited at higher magnification. Figure S4: (a) Lineweaver-Burk model of IW3 against control for xanthine oxidase inhibition assay. (b) The plot in squared area (from

0.0 mM<sup>-1</sup>–1.0 mM<sup>-1</sup> Xanthine) is exhibited at higher magnification. Figure S5: (a) Lineweaver-Burk model of VS14 against control for xanthine oxidase inhibition assay. (b) The plot in squared area (from 0.0 mM<sup>-1</sup>–1.0 mM<sup>-1</sup> Xanthine) is exhibited at higher magnification. Figure S6: Michaelis-Menten model of chosen bioactive peptides; i.e., VW4 (peptide 2), IW3 (peptide 3), and VS14 (peptide 9); against control for tyrosinase inhibition assay. The concentration of peptide used was 0.5 mg/mL. Data expressed as means ± SD of triplicates. Figure S7: Lineweaver-Burk model of VW4 against control for tyrosinase inhibition assay. (b) The plot in squared area (from 0.0 mM<sup>-1</sup>–2.0 mM<sup>-1</sup> L-tyrosine) is exhibited at higher magnification. Figure S8: (a) Lineweaver-Burk model of IW3 against control for tyrosinase inhibition assay. (b) The plot in squared area (from 0.0 mM<sup>-1</sup>–2.0 mM<sup>-1</sup> L-tyrosine) is exhibited at higher magnification. Figure S9: (a) Lineweaver-Burk model of VS14 against control for tyrosinase inhibition assay. (b) The plot in squared area (from 0.0 mM<sup>-1</sup>–2.0 mM<sup>-1</sup> L-tyrosine) is exhibited at higher magnification.

**Author Contributions:** Conceptualization, B.-S.W. and S.-M.H.; data curation, C.-Y.S. and D.-F.H.; formal analysis, A.T.; funding acquisition, S.-M.H. and T.-Y.C.; investigation, A.T., Y.-W.C., T.-C.H. and C.-Y.S.; methodology, Y.-W.C., D.-F.H. and T.-Y.C.; project administration, T.-Y.C.; supervision, B.-S.W., D.-F.H. and T.-Y.C.; validation, B.-S.W., S.-M.H. and T.-C.H.; writing—original draft, A.T.; writing—review & editing, Y.-W.C. and T.-Y.C. All authors have read and agreed to the published version of the manuscript.

**Funding:** This study was supported by funds from the University System of Taipei Joint Research Program (USTP-NTOU-TMU-106-01).

**Institutional Review Board Statement:** Not applicable.

**Informed Consent Statement:** Not applicable.

**Data Availability Statement:** Not applicable.

**Conflicts of Interest:** The authors declare that we do not have any conflict of interest.

## References

1. Chakrabarti, S.; Jahandideh, F.; Wu, J. Food-Derived Bioactive Peptides on Inflammation and Oxidative Stress. *BioMed Res. Int.* **2014**, *2014*, 608979. [[CrossRef](#)] [[PubMed](#)]
2. Halim, N.; Yusof, H.; Sarbon, N. Functional and bioactive properties of fish protein hydrolysates and peptides: A comprehensive review. *Trends Food Sci. Technol.* **2016**, *51*, 24–33. [[CrossRef](#)]
3. Chalamaiah, M.; Kumar, B.D.; Hemalatha, R.; Jyothirmayi, T. Fish protein hydrolysates: Proximate composition, amino acid composition, antioxidant activities and applications: A review. *Food Chem.* **2012**, *135*, 3020–3038. [[CrossRef](#)]
4. Kitts, D.; Weiler, D.D.K.A.K. Bioactive Proteins and Peptides from Food Sources. Applications of Bioprocesses used in Isolation and Recovery. *Curr. Pharm. Des.* **2003**, *9*, 1309–1323. [[CrossRef](#)]
5. Daliri, E.B.-M.; Lee, B.H.; Oh, D.H. Current trends and perspectives of bioactive peptides. *Crit. Rev. Food Sci. Nutr.* **2017**, *58*, 2273–2284. [[CrossRef](#)]
6. Li-Chan, E.C. Bioactive peptides and protein hydrolysates: Research trends and challenges for application as nutraceuticals and functional food ingredients. *Curr. Opin. Food Sci.* **2015**, *1*, 28–37. [[CrossRef](#)]
7. Landreh, M.; Jörnvall, H. Biological activity versus physiological function of proinsulin C-peptide. *Cell. Mol. Life Sci.* **2021**, *78*, 1131–1138. [[CrossRef](#)]
8. Jakubczyk, A.; Karaś, M.; Rybczyńska-Tkaczyk, K.; Zielińska, E.; Zieliński, D. Current Trends of Bioactive Peptides—New Sources and Therapeutic Effect. *Foods* **2020**, *9*, 846. [[CrossRef](#)] [[PubMed](#)]
9. Zamora-Sillero, J.; Gharsallaoui, A.; Prentice, C. Peptides from Fish By-product Protein Hydrolysates and Its Functional Properties: An Overview. *Mar. Biotechnol.* **2018**, *20*, 118–130. [[CrossRef](#)] [[PubMed](#)]
10. Jafarpour, A.; Gomes, R.M.; Gregersen, S.; Sloth, J.J.; Jacobson, C.; Sørensen, A.-D.M. Characterization of cod (*Gadus morhua*) frame composition and its valorization by enzymatic hydrolysis. *J. Food Compos. Anal.* **2020**, *89*, 103469. [[CrossRef](#)]
11. Sila, A.; Bougatef, A. Antioxidant peptides from marine by-products: Isolation, identification and application in food systems. A review. *J. Funct. Foods* **2016**, *21*, 10–26. [[CrossRef](#)]
12. Hajfathalian, M.; Ghelichi, S.; Moreno, P.J.G.; Sørensen, A.-D.M.; Jacobsen, C. Peptides: Production, bioactivity, functionality, and applications. *Crit. Rev. Food Sci. Nutr.* **2017**, *58*, 3097–3129. [[CrossRef](#)]
13. Tonolo, F.; Moretto, L.; Grinzato, A.; Fiorese, F.; Folda, A.; Scalcon, V.; Ferro, S.; Arrigoni, G.; Bellamio, M.; Feller, E.; et al. Fermented Soy-Derived Bioactive Peptides Selected by a Molecular Docking Approach Show Antioxidant Properties Involving the Keap1/Nrf2 Pathway. *Antioxidants* **2020**, *9*, 1306. [[CrossRef](#)]
14. Tadesse, S.A.; Emire, S.A. Production and processing of antioxidant bioactive peptides: A driving force for the functional food market. *Heliyon* **2020**, *6*, e04765. [[CrossRef](#)] [[PubMed](#)]

15. Jafarpour, A.; Gregersen, S.; Gomes, R.M.; Marcatili, P.; Olsen, T.H.; Jacobsen, C.; Overgaard, M.T.; Sørensen, A.-D.M. Biofunctionality of Enzymatically Derived Peptides from Codfish (*Gadus morhua*) Frame: Bulk In Vitro Properties, Quantitative Proteomics, and Bioinformatic Prediction. *Mar. Drugs* **2020**, *18*, 599. [[CrossRef](#)] [[PubMed](#)]
16. Minkiewicz, P.; Iwaniak, A.; Darewicz, M. BIOPEP-UWM Database of Bioactive Peptides: Current Opportunities. *Int. J. Mol. Sci.* **2019**, *20*, 5978. [[CrossRef](#)]
17. Olsen, T.H.; Yesiltas, B.; Marin, F.I.; Pertseva, M.; García-Moreno, P.J.; Gregersen, S.; Overgaard, M.T.; Jacobsen, C.; Lund, O.; Hansen, E.B.; et al. AnOxPePred: Using deep learning for the prediction of antioxidative properties of peptides. *Sci. Rep.* **2020**, *10*, 1–10. [[CrossRef](#)] [[PubMed](#)]
18. Singh, H. The milk fat globule membrane—A biophysical system for food applications. *Curr. Opin. Colloid Interface Sci.* **2006**, *11*, 154–163. [[CrossRef](#)]
19. Kathriarachchi, K.; Leus, M.; Everett, D.W. Oxidation of aldehydes by xanthine oxidase located on the surface of emulsions and washed milk fat globules. *Int. Dairy J.* **2014**, *37*, 117–126. [[CrossRef](#)]
20. Battelli, M.G.; Polito, L.; Bolognesi, A. Xanthine oxidoreductase in atherosclerosis pathogenesis: Not only oxidative stress. *Atherosclerosis* **2014**, *237*, 562–567. [[CrossRef](#)]
21. Khanna, D.; Fitzgerald, J.D.; Khanna, P.P.; Bae, S.; Singh, M.K.; Neogi, T.; Pillinger, M.H.; Merrill, J.; Lee, S.; Prakash, S.; et al. 2012 American College of Rheumatology guidelines for management of gout. Part 1: Systematic nonpharmacologic and pharmacologic therapeutic approaches to hyperuricemia. *Arthritis Rheum.* **2012**, *64*, 1431–1446. [[CrossRef](#)]
22. Li, S.; Tang, Y.; Liu, C.; Li, J.; Guo, L.; Zhang, Y. Development of a method to screen and isolate potential xanthine oxidase inhibitors from *Panax japonicus* var via ultrafiltration liquid chromatography combined with counter-current chromatography. *Talanta* **2015**, *134*, 665–673. [[CrossRef](#)]
23. Mayer, A.M. Polyphenol oxidases in plants and fungi: Going places? A review. *Phytochemistry* **2006**, *67*, 2318–2331. [[CrossRef](#)]
24. Nirmal, N.P.; Benjakul, S. Use of tea extracts for inhibition of polyphenoloxidase and retardation of quality loss of Pacific white shrimp during iced storage. *LWT* **2011**, *44*, 924–932. [[CrossRef](#)]
25. Loizzo, M.R.; Tundis, R.; Menichini, F. Natural and Synthetic Tyrosinase Inhibitors as Antibrowning Agents: An Update. *Compr. Rev. Food Sci. Food Saf.* **2012**, *11*, 378–398. [[CrossRef](#)]
26. Dai, X.-Y.; Zhang, M.-X.; Wei, X.-Y.; Hider, R.C.; Zhou, T. Novel Multifunctional Hydroxypyridinone Derivatives as Potential Shrimp Preservatives. *Food Bioprocess Technol.* **2016**, *9*, 1079–1088. [[CrossRef](#)]
27. Chen, K.; Zhao, D.-Y.; Chen, Y.-L.; Wei, X.-Y.; Li, Y.-T.; Kong, L.-M.; Hider, R.C.; Zhou, T. A Novel Inhibitor Against Mushroom Tyrosinase with a Double Action Mode and Its Application in Controlling the Browning of Potato. *Food Bioprocess Technol.* **2017**, *10*, 2146–2155. [[CrossRef](#)]
28. Demirkiran, O.; Sabudak, T.; Ozturk, M.; Topcu, G. Antioxidant and Tyrosinase Inhibitory Activities of Flavonoids from *Trifolium nigrescens* Subsp. *petrisavi*. *J. Agric. Food Chem.* **2013**, *61*, 12598–12603. [[CrossRef](#)] [[PubMed](#)]
29. Perluigi, M.; De Marco, F.; Foppoli, C.; Coccia, R.; Blarmino, C.; Marcante, M.L.; Cini, C. Tyrosinase protects human melanocytes from ROS-generating compounds. *Biochem. Biophys. Res. Commun.* **2003**, *305*, 250–256. [[CrossRef](#)]
30. Dalle-Donne, I.; Rossi, R.; Colombo, R.; Giustarini, D.; Milzani, A. Biomarkers of Oxidative Damage in Human Disease. *Clin. Chem.* **2006**, *52*, 601–623. [[CrossRef](#)]
31. Wu, H.C. Studies on bioactive peptides as related to antioxidant activities of meat essences and enzyme hydrolysates of mackerel meat. Ph.D. Thesis, National Taiwan Ocean University, Keelung, Taiwan, 2003.
32. Chou, C.-T.; Kong, Z.-L.; Shiau, C.-Y. Assessment of anti-inflammation function of Val-Trp-Trp-Trp from mackerel hydrolysates using cultured cell model. *J. Biosci. Bioeng.* **2009**, *108*, S143. [[CrossRef](#)]
33. You, L.; Zhao, M.; Regenstein, J.M.; Ren, J. Purification and identification of antioxidative peptides from loach (*Misgurnus anguillicaudatus*) protein hydrolysate by consecutive chromatography and electrospray ionization-mass spectrometry. *Food Res. Int.* **2010**, *43*, 1167–1173. [[CrossRef](#)]
34. Kumar, N.S.S.; Nazeer, R.A.; Jaiganesh, R. Purification and identification of antioxidant peptides from the skin protein hydrolysate of two marine fishes, horse mackerel (*Magalaspis cordyla*) and croaker (*Otolithes ruber*). *Amino Acids* **2011**, *42*, 1641–1649. [[CrossRef](#)] [[PubMed](#)]
35. Bougatef, A.; Nedjar-Arroume, N.; Manni, L.; Ravallec, R.; Barkia, A.; Guillochon, D.; Nasri, M. Purification and identification of novel antioxidant peptides from enzymatic hydrolysates of sardinelle (*Sardinella aurita*) by-products proteins. *Food Chem.* **2010**, *118*, 559–565. [[CrossRef](#)]
36. Je, J.-Y.; Park, P.-J.; Kim, S.-K. Antioxidant activity of a peptide isolated from Alaska pollack (*Theragra chalcogramma*) frame protein hydrolysate. *Food Res. Int.* **2005**, *38*, 45–50. [[CrossRef](#)]
37. Je, J.-Y.; Qian, Z.-J.; Byun, H.-G.; Kim, S.-K. Purification and characterization of an antioxidant peptide obtained from tuna backbone protein by enzymatic hydrolysis. *Process. Biochem.* **2007**, *42*, 840–846. [[CrossRef](#)]
38. Ren, J.; Zhao, M.; Shi, J.; Wang, J.; Jiang, Y.; Cui, C.; Kakuda, Y.; Xue, S.J. Purification and identification of antioxidant peptides from grass carp muscle hydrolysates by consecutive chromatography and electrospray ionization-mass spectrometry. *Food Chem.* **2008**, *108*, 727–736. [[CrossRef](#)]
39. Hsu, K.-C. Purification of antioxidative peptides prepared from enzymatic hydrolysates of tuna dark muscle by-product. *Food Chem.* **2010**, *122*, 42–48. [[CrossRef](#)]

40. Majumder, K.; Wu, J. A new approach for identification of novel antihypertensive peptides from egg proteins by QSAR and bioinformatics. *Food Res. Int.* **2010**, *43*, 1371–1378. [[CrossRef](#)]
41. Huang, W.; Chakrabarti, S.; Majumder, K.; Jiang, Y.; Davidge, S.T.; Wu, J. Egg-Derived Peptide IRW Inhibits TNF- $\alpha$ -Induced Inflammatory Response and Oxidative Stress in Endothelial Cells. *J. Agric. Food Chem.* **2010**, *58*, 10840–10846. [[CrossRef](#)]
42. Liao, W.; Chakrabarti, S.; Davidge, S.T.; Wu, J. Modulatory Effects of Egg White Ovotransferrin-Derived Tripeptide IRW (Ile-Arg-Trp) on Vascular Smooth Muscle Cells against Angiotensin II Stimulation. *J. Agric. Food Chem.* **2016**, *64*, 7342–7347. [[CrossRef](#)] [[PubMed](#)]
43. Son, M.; Wu, J. Egg white hydrolysate and peptide reverse insulin resistance associated with tumor necrosis factor- $\alpha$  (TNF- $\alpha$ ) stimulated mitogen-activated protein kinase (MAPK) pathway in skeletal muscle cells. *Eur. J. Nutr.* **2019**, *58*, 1961–1969. [[CrossRef](#)]
44. Liu, G.; Yan, W.; Ding, S.; Jiang, H.; Ma, Y.; Wang, H.; Fang, J. Effects of IRW and IQW on Oxidative Stress and Gut Microbiota in Dextran Sodium Sulfate-Induced Colitis. *Cell. Physiol. Biochem.* **2018**, *51*, 441–451. [[CrossRef](#)]
45. Ma, Y.; Ding, S.; Liu, G.; Fang, J.; Yan, W.; Duraipandiyar, V.; Al-Dhabi, N.A.; Esmail, G.A.; Jiang, H. Egg Protein Transferrin-Derived Peptides IRW and IQW Regulate Citrobacter rodentium-Induced, Inflammation-Related Microbial and Metabolomic Profiles. *Front. Microbiol.* **2019**, *10*, 643. [[CrossRef](#)]
46. Liao, W.; Fan, H.; Davidge, S.T.; Wu, J. Egg White-Derived Antihypertensive Peptide IRW (Ile-Arg-Trp) Reduces Blood Pressure in Spontaneously Hypertensive Rats via the ACE2/Ang (1-7)/Mas Receptor Axis. *Mol. Nutr. Food Res.* **2019**, *63*, 1900063. [[CrossRef](#)]
47. Alam, N.; Bristi, N.J. Rafiquzzaman Review on in vivo and in vitro methods evaluation of antioxidant activity. *Saudi Pharm. J.* **2013**, *21*, 143–152. [[CrossRef](#)] [[PubMed](#)]
48. Sheih, I.-C.; Wu, T.-K.; Fang, T.J. Antioxidant properties of a new antioxidative peptide from algae protein waste hydrolysate in different oxidation systems. *Bioresour. Technol.* **2009**, *100*, 3419–3425. [[CrossRef](#)]
49. Cian, R.E.; Martínez-Augustin, O.; Drago, S.R. Bioactive properties of peptides obtained by enzymatic hydrolysis from protein byproducts of *Porphyra columbina*. *Food Res. Int.* **2012**, *49*, 364–372. [[CrossRef](#)]
50. Noro, T.; Oda, Y.; Miyase, T.; Ueno, A.; Fukushima, S. Inhibitors of xanthine oxidase from the flowers and buds of *Daphne genkwa*. *Chem. Pharm. Bull.* **1983**, *31*, 3984–3987. [[CrossRef](#)] [[PubMed](#)]
51. Takagi, K.; Mitsunaga, T. Tyrosinase inhibitory activity of proanthocyanidins from woody plants. *J. Wood Sci.* **2003**, *49*, 461–465. [[CrossRef](#)]
52. Sae-Leaw, T.; Karnjanapratum, S.; O’Callaghan, Y.C.; O’Keeffe, M.B.; Fitzgerald, R.J.; O’Brien, N.M.; Benjakul, S. Purification and identification of antioxidant peptides from gelatin hydrolysate of seabass skin. *J. Food Biochem.* **2016**, *41*, e12350. [[CrossRef](#)]
53. Elias, R.J.; McClements, D.J.; Decker, E.A. Antioxidant Activity of Cysteine, Tryptophan, and Methionine Residues in Continuous Phase  $\beta$ -Lactoglobulin in Oil-in-Water Emulsions. *J. Agric. Food Chem.* **2005**, *53*, 10248–10253. [[CrossRef](#)]
54. Ashaolu, T.J. Antioxidative peptides derived from plants for human nutrition: Their production, mechanisms and applications. *Eur. Food Res. Technol.* **2020**, *246*, 853–865. [[CrossRef](#)]
55. Chen, H.-M.; Muramoto, K.; Yamauchi, F.; Fujimoto, K.; Nokihara, K. Antioxidative Properties of Histidine-Containing Peptides Designed from Peptide Fragments Found in the Digests of a Soybean Protein. *J. Agric. Food Chem.* **1998**, *46*, 49–53. [[CrossRef](#)]
56. Yang, Q.; Cai, X.; Yan, A.; Tian, Y.; Du, M.; Wang, S. A specific antioxidant peptide: Its properties in controlling oxidation and possible action mechanism. *Food Chem.* **2020**, *327*, 126984. [[CrossRef](#)] [[PubMed](#)]
57. Ajibola, C.F.; Fashakin, J.B.; Fagbemi, T.N.; Aluko, R.E. Effect of Peptide Size on Antioxidant Properties of African Yam Bean Seed (*Sphenostylis stenocarpa*) Protein Hydrolysate Fractions. *Int. J. Mol. Sci.* **2011**, *12*, 6685–6702. [[CrossRef](#)]
58. Qian, Z.-J.; Jung, W.-K.; Kim, S.-K. Free radical scavenging activity of a novel antioxidative peptide purified from hydrolysate of bullfrog skin, *Rana catesbeiana* Shaw. *Bioresour. Technol.* **2008**, *99*, 1690–1698. [[CrossRef](#)]
59. You, L.; Zhao, M.; Cui, C.; Zhao, H.; Yang, B. Effect of degree of hydrolysis on the antioxidant activity of loach (*Misgurnus anguillicaudatus*) protein hydrolysates. *Innov. Food Sci. Emerg. Technol.* **2009**, *10*, 235–240. [[CrossRef](#)]
60. Nongonierma, A.B.; Fitzgerald, R.J. Tryptophan-containing milk protein-derived dipeptides inhibit xanthine oxidase. *Peptides* **2012**, *37*, 263–272. [[CrossRef](#)] [[PubMed](#)]
61. Li, Q.; Kang, X.; Shi, C.; Li, Y.; Majumder, K.; Ning, Z.; Ren, J. Moderation of hyperuricemia in rats via consuming walnut protein hydrolysate diet and identification of new antihyperuricemic peptides. *Food Funct.* **2017**, *9*, 107–116. [[CrossRef](#)]
62. Li, Q.; Shi, C.; Wang, M.; Zhou, M.; Liang, M.; Zhang, T.; Yuan, E.; Wang, Z.; Yao, M.; Ren, J. Tryptophan residue enhances in vitro walnut protein-derived peptides exerting xanthine oxidase inhibition and antioxidant activities. *J. Funct. Foods* **2019**, *53*, 276–285. [[CrossRef](#)]
63. Rashidinejad, A.; Birch, J. Xanthine Oxidase in Dairy Foods. *Encycl. Food Chem.* **2019**, 374–380. [[CrossRef](#)]
64. Sha, W.; Hou, C.; Yuan, E.; Li, Y.; Ren, J. Different processed milk with residual xanthine oxidase activity and risk of increasing serum uric acid level. *Food Biosci.* **2021**, *40*, 100892. [[CrossRef](#)]
65. Masuda, T.; Fukuyama, Y.; Doi, S.; Masuda, A.; Kurosawa, S.; Fujii, S.; Kurosawa, S. Effects of Temperature on the Composition and Xanthine Oxidase Inhibitory Activities of Caffeic Acid Roasting Products. *J. Agric. Food Chem.* **2019**, *67*, 8977–8985. [[CrossRef](#)] [[PubMed](#)]
66. Zhong, H.; Abdullah; Zhang, Y.; Deng, L.; Zhao, M.; Tang, J.; Zhang, H.; Feng, F.; Wang, J. Exploring the Potential of Novel Xanthine Oxidase Inhibitory Peptide (ACECD) Derived from Skipjack Tuna Hydrolysates Using Affinity-Ultrafiltration Coupled with HPLC–MALDI-TOF/TOF-MS. *Food Chem.* **2021**, *347*, 129068. [[CrossRef](#)] [[PubMed](#)]

- 
67. Bu, Y.; Wang, F.; Zhu, W.; Li, X. Combining bioinformatic prediction and assay experiment to identify novel xanthine oxidase inhibitory peptides from Pacific bluefin tuna (*Thunnus orientalis*). *E3S Web Conf.* **2020**, *185*, 04062. [[CrossRef](#)]
  68. Chang, T.-S. An Updated Review of Tyrosinase Inhibitors. *Int. J. Mol. Sci.* **2009**, *10*, 2440–2475. [[CrossRef](#)]
  69. Zolghadri, S.; Bahrami, A.; Khan, M.T.H.; Munoz-Munoz, J.; Garcia-Molina, F.; Garcia-Canovas, F.; Saboury, A.A. A comprehensive review on tyrosinase inhibitors. *J. Enzym. Inhib. Med. Chem.* **2019**, *34*, 279–309. [[CrossRef](#)]